Chapter 2

Study of collinear cracks in a composite medium subjected to time-harmonic wave disturbance

2.1 Introduction

During the last few decades the composite materials which are made from two or more constituent materials having different physical properties and possesses different characteristics from individual components have been used by the engineers in air crafts, bridges, automobiles, bullet trains, spacecrafts etc., for its high strength and light weight. Most of the composite materials are made by one material with the reinforcement of fragments of stronger materials. There is flexibility of various choices in the manufacturing process to determine what should be the properties of the resulting composite. The primary demand of composite materials has been created by the modern aviation. There are a lot of reasons for growing up the applications of composites, but the primary one is the products made by composite are stronger and lighter. Metal loses its strength when the temperature is evaluated. High polymeric material can resist lower temperature. Ceramic can replace metal and polymer as it can resist at high temperature due to its thermal expansion property and strength. But due to the brittleness it is often treated unacceptable as structural material. Thus there is a need of composites.

The researchers working in the area of composite materials are concerned with the damage mechanics of the composites with the help of different mechanism.The damage caused due to thermo-mechanical loadings and their effects on the failure and fatigue behaviours of the composite structure are also considered. Due to the increasing use of composites in the aircraft structures, the researchers are focused to

understand the performance of composite materials and its structures under different flight loads. The failure and fracture analyses of these materials are very much needed to avoid aircraft accident. The orthotropic materials are useful to deal with the fracture problems in composite materials.Due to the high module, high strength and low weight, the orthotropic composites are frequently used in high speed aircrafts, missiles, rocket engines, satellites etc. The most growing example of utilization of orthotropic composite in spacecraft applications is due to its weight savings and dimensional stability.

Thus the presence of cracks may cause premature failure of structures. Several problems related to crack propagation of constant speed have been studied in fracture mechanics for orthotropic materials.It is found from the literature survey that many researchers have contributed the problem of crack/cracks in orthotropic media [55–65]. Itou [66] has studied the problem of two co-planer Griffith cracks situated in an orthotropic elastic layer sandwiched between two isotropic half-planes while Das et. al. [67] have studied the sandwiched problem of two co-planer Griffith cracks which has further been solved by converting the problem into integral equations.Das and Patra [68] have studied the problem of three co-planer Griffith cracks located symmetrically in the mid-plane of an orthotropic elastic layer of finite length. In 2003, Das and Debnath [69] have investigated the interactions between Griffith cracks in sandwiched orthotropic layer using Fourier transform technique and showed that the effects are either shielding or amplification depending on the location of cracks, shaping of crack-tips and thickness of the layers.Recently Liu et. al. [70]have determined stress intensity factors for two unequal collinear cracks using weight function method. A simple and accurate method has been presented for computing SIF of collinear interacting cracks by Millwater [71]. Ohyoshi [72] considered the diffraction of P and SV-waves by a finite crack situated in orthotropic medium and studied the orthotropic effect on singular stress components while Kassir and Bandyopadhyay [33] determined the elastodynamic response of an orthotropic solid containing a crack under the action of normal impact loading. In both the studies peak values of dynamic SIFs have been obtained. The problem of two collinear cracks in an orthotropic plate has been studied by Sarkar et al. [73]. Lira-Vergara and Rubio Gonzalez [64] calculated the SIFs of a crack situated on an interface of dissimilar orthotropic half-planes. Later, Itou [66, 74] studied the problem of two collinear cracks in the presence of time-harmonic waves and reported the peak values of SIFs. Recently, Singh et al. [75] have calculated the analytical expressions of SIFs of an interfacial crack in an orthotropic strip under the normal and shear impact loadings and provided the peak values of dynamic SIFs. In 2016, Itou [76]

has determined the dynamic SIFs of three collinear cracks in an orthotropic medium subjected to time-harmonic disturbance.

Plane wave is an example of a time harmonic field where the time variation is considered as sinusoidal. The waves are described as disturbances during travel through media, which are transporting energy from one location to another without transporting matter. The simple disturbance as a wave function is considered as sine function which is conveyed in medium to generate harmonic waves. It is assumed that for the rigid wall the normal stress to the wall is zero, but for the interface it becomes complicated and defined by a complex quantity for the linear independence.The quantity is defined by the ratio of stresses imposed to the normal velocity to the surface where both the terms include a harmonic time dependence $e^{-i\omega t}$.Thus there is a primary importance in harmonic wave behaviour in analytical sense since any form of time dependence is continued and analysed into a set of functions.

This chapter is oriented towards the investigations of SIFs at the tips of three collinear cracks in a sandwiched orthotropic strip and also the shielding and amplification of central crack due to the presence of outer cracks through stress magnification factor. To find the solution, the whole problem has been transformed into Fourier transformed plane. The Schmidt method [77] has been used to find the unknowns.Approximate analytical expressions of SIFs at cracks' tips have been derived.The variations of normalised SIFs and SMF against different wave numbers, due to various lengths of the cracks and depths of the strip are displayed graphically.

2.2 Mathematical formulation

Let us consider an orthotropic composite material made with a semi-infinite orthotropic strip as medium 1 ($-\infty < x < \infty, -h \leq y \leq h$) which is bounded between two identical orthotropic half-planes as medium 2 ($-\infty < x < \infty, h \leq y < \infty; -\infty < x < \infty, -\infty < y \leq -h$).The strip is weakened by three cracks situated symmetrically at the mid-plane of the strip, in which the length of the central crack is 2a and each of the outer crack is (c-b) as shown through the Fig.2.1.It is considered that the cracks ($|x| < a$, $b < |x| < c$) are subjected to the time-harmonic waves and fulfil the symmetric requirements.

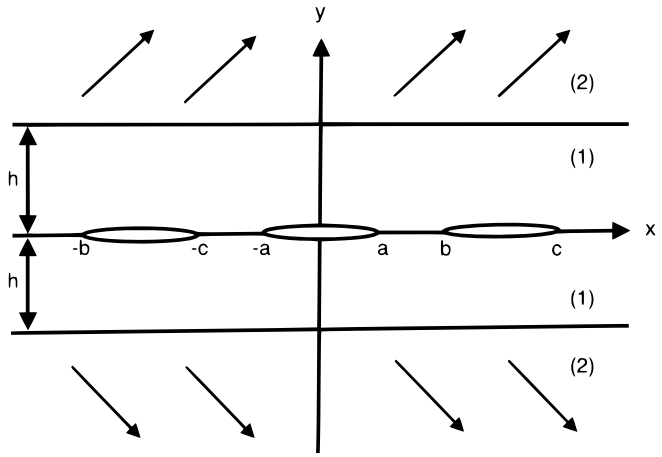

Figure 2.1: Geometry of the problem

The equations of motion for the considered model are given by

$$C_{11}^{(j)}\frac{\partial^2 U^{(j)}}{\partial x^2}+\frac{\partial^2 U^{(j)}}{\partial y^2}+\left(1+C_{12}^{(j)}\right)\frac{\partial^2 V^{(j)}}{\partial x\partial y}=\frac{1}{C_T^{(j)2}}\frac{\partial^2 U^{(j)}}{\partial t^2},$$
$$\frac{\partial^2 V^{(j)}}{\partial x^2}+C_{22}^{(j)}\frac{\partial^2 V^{(j)}}{\partial y^2}+\left(1+C_{12}^{(j)}\right)\frac{\partial^2 U^{(j)}}{\partial x\partial y}=\frac{1}{C_T^{(j)2}}\frac{\partial^2 V^{(j)}}{\partial t^2}, \qquad (2.2.1)$$

where $U^{(j)}(x,y,t)$ and $V^{(j)}(x,y,t)$ are displacement components along x and y directions respectively, $C_{ik}^{(j)}$'s are elastic constants, $C_T^{(j)}=(C_{66}^{(j)}/\rho^{(j)})^{1/2}$ are frequency ratios and $j=1,2$ refer to the strip 1 and half-plane 2 respectively.

The stress components are

$$\tau_{yy}^{(j)}/C_{66}^{(j)}=\left(C_{12}^{(j)}\frac{\partial U^{(j)}}{\partial x}+C_{22}^{(j)}\frac{\partial V^{(j)}}{\partial y}\right),$$
$$\tau_{xy}^{(j)}/C_{66}^{(j)}=\frac{\partial U^{(j)}}{\partial y}+\frac{\partial V^{(j)}}{\partial x}. \qquad (2.2.2)$$

Let the incident elastic wave is impinging on the surface of the cracks from the normal direction.Therefore the displacement components are considered as

$$U^{(1)}=0\,,$$
$$V^{(1)}=A\,\exp\left(i\omega y/(C_T^{(1)}\sqrt{C_{22}^{(1)}})+i\omega t\right), \qquad (2.2.3)$$

where A and ω are amplitude and circular frequency of the time-harmonic wave. From Eqs (2.2.2) and (2.2.3), we get

$$\begin{aligned} \tau_{yy}^{(1)}/C_{66}^{(1)} &= p\,\exp\left(i\omega y/(C_T^{(1)}\sqrt{C_{22}^{(1)}}) + i\omega t\right), \\ \tau_{xy}^{(1)} &= 0, \end{aligned} \tag{2.2.4}$$

where $p = A\,C_{22}^{(1)}\omega i/(C_T^{(1)}\sqrt{C_{22}^{(1)}})$.

Substituting $U^{(j)}(x,y,t) = u^{(j)}(x,y)\,e^{i\omega t}$ and $V^{(j)}(x,y,t) = v^{(j)}(x,y)\,e^{i\omega t}$ in Eq.(2.2.1) , we get

$$\begin{aligned} &C_{11}^{(j)}\frac{\partial^2 u^{(j)}}{\partial x^2} + \frac{\partial^2 u^{(j)}}{\partial y^2} + \left(1 + C_{12}^{(j)}\right)\frac{\partial^2 v^{(j)}}{\partial x \partial y} + \frac{\omega^2}{C_T^{(j)2}}u^{(j)} = 0, \\ &\frac{\partial^2 v^{(j)}}{\partial x^2} + C_{22}^{(j)}\frac{\partial^2 v^{(j)}}{\partial y^2} + \left(1 + C_{12}^{(j)}\right)\frac{\partial^2 u^{(j)}}{\partial x \partial y} + \frac{\omega^2}{C_T^{(j)2}}v^{(j)} = 0, j = 1, 2. \end{aligned} \tag{2.2.5}$$

The corresponding stresses are given by

$$\begin{aligned} \sigma_{yy}^{(j)} &= C_{66}^{(j)}\left(C_{12}^{(j)}\frac{\partial u^{(j)}}{\partial x} + C_{22}^{(j)}\frac{\partial v^{(j)}}{\partial y}\right), \\ \sigma_{xy}^{(j)} &= \frac{\partial u^{(j)}}{\partial y} + \frac{\partial v^{(j)}}{\partial x}. \end{aligned} \tag{2.2.6}$$

where $\sigma_{yy}^{(j)} = \tau_{yy}^{(j)}\,e^{-i\omega t}$ and $\sigma_{xy}^{(j)} = \tau_{xy}^{(j)}\,e^{-i\omega t}$.

The boundary and continuity conditions for the considered mathematical model are given as follows:
On $y = 0$,

$$\sigma_{yy}^{(1)}(x,0) = -p, \qquad |x| \le a,\ b \le |x| \le c, \tag{2.2.7}$$

$$\sigma_{xy}^{(1)}(x,0) = 0, \qquad |x| < \infty, \tag{2.2.8}$$

$$v^{(1)}(x,0) = 0, \qquad a < |x| < b,\ |x| > c. \tag{2.2.9}$$

On $y = h$,

$$\sigma_{yy}^{(1)}(x,h) = \sigma_{yy}^{(2)}(x,h), \qquad |x| < \infty, \tag{2.2.10}$$

$$\sigma_{xy}^{(1)}(x,h) = \sigma_{xy}^{(2)}(x,h), \qquad |x| < \infty, \tag{2.2.11}$$

$$u^{(1)}(x,h) = u^{(2)}(x,h), \qquad |x| < \infty, \tag{2.2.12}$$

$$v^{(1)}(x,h) = v^{(2)}(x,h), \qquad |x| < \infty. \tag{2.2.13}$$

The components of the stresses vanish from the remote distance of the cracks.

2.3 Solution of the problem

Applying the Fourier transformation from Eq.(1.4.1), the Eqs (2.2.5) are reduced in the following form as

$$\left(\frac{\partial^4}{\partial y^4} + q_j \frac{\partial^2}{\partial y^2} + r_j\right)\left(\overline{u}^{(j)}, \overline{v}^{(j)}\right) = 0, \quad j = 1, 2, \tag{2.3.1}$$

where

$$q_j = \zeta^2(2C_{12}^{(j)} - C_{11}^{(j)}C_{22}^{(j)} + C_{12}^{(j)2})/C_{22}^{(j)} + (1 + C_{22}^{(j)})\frac{\omega^2}{C_{22}^{(j)}C_T^{(j)2}},$$

$$r_j = \left(\zeta^2 C_{11}^{(j)} - \frac{\omega^2}{C_T^{(j)2}}\right)\left(\zeta^2 - \frac{\omega^2}{C_T^{(j)2}}\right)/C_{22}^{(j)} \tag{2.3.2}$$

The expressions of the solutions of the Eq.(2.3.1) are assumed as

$$\begin{aligned}\overline{u}^{(1)}(\zeta, y) = {} & A^{(1)}(\zeta)\exp(\gamma_1^{(1)}y) + B^{(1)}(\zeta)\exp(-\gamma_1^{(1)}y) \\ & + C^{(1)}(\zeta)\exp(\gamma_2^{(1)}y) + D^{(1)}(\zeta)\exp(-\gamma_2^{(1)}y),\end{aligned} \tag{2.3.3}$$

$$\begin{aligned}\overline{v}^{(1)}(\zeta, y) = {} & \alpha_1^{(1)}A^{(1)}(\zeta)\exp(\gamma_1^{(1)}y) - \alpha_1^{(1)}B^{(1)}(\zeta)\exp(-\gamma_1^{(1)}y) \\ & + \alpha_2^{(1)}C^{(1)}(\zeta)\exp(\gamma_2^{(1)}y) - \alpha_2^{(1)}D^{(1)}(\zeta)\exp(-\gamma_2^{(1)}y),\end{aligned} \tag{2.3.4}$$

$$\overline{u}^{(2)}(\zeta, y) = A^{(2)}(\zeta)\exp(-\gamma_1^{(2)}y) + B^{(2)}(\zeta)\exp(-\gamma_2^{(2)}y),$$

$$\overline{v}^{(2)}(\zeta, y) = -\alpha_1^{(2)}A^{(2)}(\zeta)\exp(-\gamma_1^{(2)}y) - \alpha_2^{(2)}B^{(2)}(\zeta)\exp(-\gamma_2^{(2)}y),$$

where $\gamma_1^{(j)}$ and $\gamma_2^{(j)}$ are the positive roots of the equations $\gamma^{(j)4} + q_j\gamma^{(j)2} + r_j = 0$, and

$\alpha_k^{(j)} = \left(\frac{\gamma_k^{(j)2} - \zeta^2 C_{11}^{(j)} + \omega^2/(C_T^{(j)2})}{i\zeta(1+C_{12}^{(j)})\gamma_k^{(j)}} \right)$ with $k = 1,\ 2;\ j = 1,\ 2.$

The expressions of stresses in the medium 1 and medium 2 are obtained as

$$\begin{aligned}\overline{\sigma}_{yy}^{(1)}(\zeta,\ y) &= i\zeta C_{66}^{(1)} C_{12}^{(1)} (A^{(1)} \exp(\gamma_1^{(1)} y) + B^{(1)} \exp(-\gamma_1^{(1)} y) + C^{(1)} \exp(\gamma_2^{(1)} y) \\ &+ D^{(1)} \exp(-\gamma_2^{(1)} y)) + C_{66}^{(1)} C_{22}^{(1)} (\alpha_1^{(1)} \gamma_1^{(1)} A^{(1)} \exp(\gamma_1^{(1)} y) \\ &+ \alpha_1^{(1)} \gamma_1^{(1)} B^{(1)} \exp(-\gamma_1^{(1)} y) + \alpha_2^{(1)} \gamma_2^{(1)} C^{(1)} \exp(\gamma_2^{(1)} y) \\ &+ \alpha_2^{(1)} \gamma_2^{(1)} D^{(1)} \exp(-\gamma_2^{(1)} y)), \end{aligned} \tag{2.3.5}$$

$$\begin{aligned}\overline{\sigma}_{xy}^{(1)}(\zeta,\ y) &= (\gamma_1^{(1)} A^{(1)} \exp(\gamma_1^{(1)} y) - \gamma_1^{(1)} B^{(1)} \exp(-\gamma_1^{(1)} y) + \gamma_2^{(1)} C^{(1)} \exp(\gamma_2^{(1)} y) \\ &- \gamma_2^{(1)} D^{(1)} \exp(-\gamma_2^{(1)} y)) + i\zeta(\alpha_1^{(1)} A^{(1)} \exp(\gamma_1^{(1)} y) - \alpha_1^{(1)} B^{(1)} \exp(-\gamma_1^{(1)} y) \\ &+ \alpha_2^{(1)} C^{(1)} \exp(\gamma_2^{(1)} y) - \alpha_2^{(1)} D^{(1)} \exp(-\gamma_2^{(1)} y)), \end{aligned} \tag{2.3.6}$$

$$\begin{aligned}\overline{\sigma}_{yy}^{(2)}(\zeta,\ y) &= i\zeta C_{66}^{(2)} C_{12}^{(2)} \left(A_k^{(2)} \exp(-\gamma_1^{(2)} y) + B_k^{(2)} \exp(-\gamma_2^{(2)} y) \right) + \\ &+ C_{66}^{(2)} C_{22}^{(2)} \left(\alpha_1^{(2)} \gamma_1^{(2)} A_k^{(2)} \exp(-\gamma_1^{(2)} y) + \alpha_2^{(2)} \gamma_2^{(2)} B_k^{(2)} \exp(-\gamma_2^{(2)} y) \right), \end{aligned} \tag{2.3.7}$$

$$\begin{aligned}\overline{\sigma}_{xy}^{(2)}(\zeta,\ y) &= \left(\gamma_1^{(2)} A^{(2)} \exp(-\gamma_1^{(2)} y) - \gamma_2^{(2)} B^{(2)} \exp(-\gamma_2^{(2)} y) \right) \\ &+ i\zeta \left(\alpha_1^{(2)} A^{(2)} \exp(-\gamma_1^{(2)} y) - \alpha_2^{(2)} B^{(2)} \exp(-\gamma_2^{(2)} y) \right). \end{aligned} \tag{2.3.8}$$

Using boundary conditions (2.2.10) - (2.2.13), we get

$$B^{(1)}(\zeta) = a_4 \exp(2\gamma_1^{(1)} h) A^{(1)}(\zeta), \tag{2.3.9}$$

$$C^{(1)}(\zeta) = b_4 \exp((\gamma_1^{(1)} - \gamma_2^{(1)}) h) A^{(1)}(\zeta), \tag{2.3.10}$$

$$D^{(1)}(\zeta) = c_4 \exp((\gamma_1^{(1)} + \gamma_2^{(1)}) h) A^{(1)}(\zeta), \tag{2.3.11}$$

$$A^{(2)}(\zeta) = [(1 - a_4) t_1 + (b_4 - c_4) t_2] \exp((\gamma_1^{(1)} + \gamma_1^{(2)}) h) A^{(1)}(\zeta), \tag{2.3.12}$$

$$B^{(2)}(\zeta) = [(1 - a_4) t_3 + (b_4 - c_4) t_4] \exp((\gamma_1^{(1)} + \gamma_2^{(2)}) h) A^{(1)}(\zeta), \tag{2.3.13}$$

where

$$a_4 = \frac{[(a_2 d_3 + a_3 b_2)(c_1 b_2 + b_2 d_1) - (a_1 b_2 + a_2 d_1)(b_2 d_3 + c_3 b_2)]}{[(b_1 b_2 - a_2 d_1)(b_2 d_3 - c_3 b_2) - (b_2 b_3 - a_2 d_3)(c_1 b_2 + b_2 d_1)]},$$

$$b_4 = -\frac{[(a_1 b_2 + a_1 d_1) - (b_1 b_2 - a_2 d_2) a]}{(c_1 b_2 + b_2 d_1)},\ c_4 = -\left(\frac{a_1}{d_1} + \frac{b_1 a}{d_1} + \frac{c_1 b}{d_1} \right),$$

$$a_1 = 1 - t_1 - t_3,\ b_1 = 1 + t_1 + t_3\ , c_1 = 1 - t_2 - t_4,\ d_1 = 1 + t_2 + t_4,$$

$$a_2 = \alpha_1^{(1)} + \alpha_1^{(2)} t_1 + \alpha_2^{(2)} t_3, \qquad b_2 = \alpha_2^{(1)} + \alpha_1^{(2)} t_2 + \alpha_2^{(2)} t_4,$$

$$a_3 = i\zeta C_{12}^{(1)} + C_{22}^{(1)} \alpha_1^{(1)} y_1^{(1)} - (i\zeta C_{12}^{(2)} + C_{22}^{(2)} \alpha_1^{(2)} \gamma_1^{(2)}) t_1 - (i\zeta C_{12}^{(2)} + C_{22}^{(2)} \alpha_2^{(2)} \gamma_2^{(2)}) t_3,$$

$$b_3 = i\zeta C_{12}^{(1)} + C_{22}^{(1)} \alpha_1^{(1)} y_1^{(1)} + (i\zeta C_{12}^{(2)} + C_{22}^{(2)} \alpha_1^{(2)} \gamma_1^{(2)}) t_1 + (i\zeta C_{12}^{(2)} + C_{22}^{(2)} \alpha_2^{(2)} \gamma_2^{(2)}) t_3,$$

$$c_3 = i\zeta C_{12}^{(1)} + C_{22}^{(1)} \alpha_1^{(1)} y_1^{(1)} - (i\zeta C_{12}^{(2)} + C_{22}^{(2)} \alpha_1^{(2)} \gamma_1^{(2)}) t_2 - (i\zeta C_{12}^{(2)} + C_{22}^{(2)} \alpha_2^{(2)} \gamma_2^{(2)}) t_4,$$

$$d_3 = i\zeta C_{12}^{(1)} + C_{22}^{(1)} \alpha_1^{(1)} y_1^{(1)} + (i\zeta C_{12}^{(2)} + C_{22}^{(2)} \alpha_1^{(2)} \gamma_1^{(2)}) t_2 + (i\zeta C_{12}^{(2)} + C_{22}^{(2)} \alpha_2^{(2)} \gamma_2^{(2)}) t_4,$$

$$t_1 = \frac{\left(\alpha_1^{(1)} \gamma_2^{(1)} - \alpha_2^{(2)} \gamma_1^{(1)}\right)}{(\alpha_2^{(2)} \gamma_1^{(2)} - \alpha_1^{(2)} \gamma_2^{(2)})}, \; t_2 = \frac{\left(\alpha_2^{(1)} \gamma_2^{(2)} - \alpha_2^{(2)} \gamma_2^{(1)}\right)}{(\alpha_2^{(2)} \gamma_1^{(2)} - \alpha_1^{(2)} \gamma_2^{(2)})},$$
$$t_3 = \frac{\left(\alpha_1^{(2)} \gamma_1^{(1)} - \alpha_1^{(1)} \gamma_1^{(2)}\right)}{(\alpha_2^{(2)} \gamma_1^{(2)} - \alpha_1^{(2)} \gamma_2^{(2)})}, \; t_4 = \frac{\left(\alpha_1^{(2)} \gamma_2^{(1)} - \alpha_2^{(1)} \gamma_1^{(2)}\right)}{(\alpha_2^{(2)} \gamma_1^{(2)} - \alpha_1^{(2)} \gamma_2^{(2)})}.$$

The boundary conditions(2.2.7) - (2.2.9) and the stress expressions give rise to

$$\sigma_{yy}^{(1)}(x,0)/C_{66}^{(1)} = \frac{1}{\pi} \int_0^\infty \overline{v}^{(1)}(\zeta,0) R(\zeta) \cos(\zeta x) d\zeta = -p/C_{66}^{(1)}, \;\; 0 \le x \le a, \; b \le x \le c, \tag{2.3.14}$$

$$v^{(1)}(x,0) = \frac{1}{\pi} \int_0^\infty \overline{v}^{(1)}(\zeta,0) \cos(\zeta x) d\zeta, \quad a < x < b, \; x > c, \tag{2.3.15}$$

where

$$\begin{aligned} R(\zeta) = {} & (\exp(-2\gamma_1^{(1)} h)(i\zeta C_{12}^{(1)} + C_{22}^{(1)} \alpha_1^{(1)} \gamma_1^{(1)}) + a_4 (i\zeta C_{12}^{(1)} + C_{22}^{(1)} \alpha_1^{(1)} \gamma_1^{(1)}) + b_4 \exp(-(\gamma_1^{(1)} \\ & + \gamma_2^{(1)}) h)(i\zeta C_{12}^{(1)} + C_{22}^{(1)} \alpha_2^{(1)} \gamma_2^{(1)}) + c_4 \exp(-(\gamma_1^{(1)} - \gamma_2^{(1)}) h)(i\zeta C_{12}^{(1)} + C_{22}^{(1)} \alpha_2^{(1)} \gamma_2^{(1)})) \\ & / (\alpha_1^{(1)} \exp(-2\gamma_1^{(1)} h) - a_4 \alpha_1^{(1)} + b_4 \alpha_2^{(1)} \exp(-(\gamma_1^{(1)} + \gamma_2^{(1)}) h) - c_4 \alpha_2^{(1)} \exp(-(\gamma_1^{(1)} \\ & - \gamma_2^{(1)}) h)). \end{aligned} \tag{2.3.16}$$

Let us suppose $v^{(1)}(x,0)$ be represented by the following series as

$$\begin{aligned} \pi C_{66}^{(1)} v^{(1)}(x,0) &= \sum_{n=1}^{\infty} a_n^{(1)} \cos\{(2n-1) \sin^{-1}(x/a)\}, \;\; 0 < x < a, \\ &= \sum_{n=1}^{\infty} \frac{b_n^{(1)}}{2n} \sin[n \sin^{-1}\{\frac{(c+b-2x)}{(c-b)}\} - \frac{n\pi}{2}], \;\; b < x < c, \\ &= 0, \qquad\qquad elsewhere. \end{aligned} \tag{2.3.17}$$

Here the condition (2.3.15) is satisfied.Applying Fourier transformation on the Eqs

(2.3.17), we get

$$C_{66}^{(1)}\overline{v}^{(1)}(\zeta,0) = \sum_{n=1}^{\infty} a_n^{(1)}(2n-1)/\xi J_{2n}(c\zeta) + \sum_{n=1}^{\infty} b_n^{(1)}(1/\xi)\sin\{(b+c)\zeta/2 - n\pi/2\}J_n\{(c-b)\zeta/2\}, \tag{2.3.18}$$

where the unknown coefficients $a_n^{(1)}$ and $b_n^{(1)}$ are to be determined and $J_n(\zeta)$ is the Bessel function. Now Eq.(2.3.14) can be rewritten as

$$\sigma_{yy}^{(1)}(x,0) = \sum_{n=1}^{\infty} a_n^{(1)}(2n-1)/\pi \int_0^{\infty} \frac{R(\zeta)}{\zeta} J_{2n-1}(c\zeta)\cos(\zeta x)d\zeta + \sum_{n=1}^{\infty} b_n^{(1)}(1/\pi)\int_0^{\infty} \frac{R(\zeta)}{\zeta}\sin\{\frac{(c+b)\zeta)}{2} - \frac{n\pi}{2}\}J_n\{\frac{(c+b)\zeta)}{2}\}\cos(\zeta x)d\zeta = -p. \tag{2.3.19}$$

The above expression can be reduced to the following forms

$$\sum_{n=1}^{\infty} a_n^{(1)}E_n^{(1)}(x) + \sum_{n=1}^{\infty} b_n^{(1)}F_n^{(1)}(x) = -p, \quad 0 \le x < a, \tag{2.3.20}$$

$$\sum_{n=1}^{\infty} a_n^{(1)}G_n^{(1)}(x) + \sum_{n=1}^{\infty} b_n^{(1)}H_n^{(1)}(x) = -p, \quad b < x < c, \tag{2.3.21}$$

where

$$E_n^{(1)}(x) = G_n^{(1)}(x) = \frac{(2n-1)}{\pi}\int_0^{\infty} \frac{R(\zeta)}{\zeta} J_{2n-1}(c\zeta)\cos(\zeta x)d\zeta,$$
$$F_n^{(1)}(x) = H_n^{(1)}(x) = \frac{1}{\pi}\int_0^{\infty} \frac{R(\zeta)}{\zeta}\sin\left(\zeta\frac{(c+b)}{2} - \frac{n\pi}{2}\right)J_{2n}\left(\zeta\frac{(c-b)}{2}\right)\cos(\zeta x)d\zeta. \tag{2.3.22}$$

To find the coefficients $a_n^{(1)}$ and $b_n^{(1)}$, we use Schmidt method [77].First consider both the equations are in $0 < x < c$. Then Eqs (2.3.20) and (2.3.21) can be written in the following forms as

$$\sum_{n=1}^{\infty} a_n^{(1)}E_n^{(1)}(x) + \sum_{n=1}^{\infty} b_n^{(1)}F_n^{(1)}(x) = -p, \quad 0 < x < c\,, \tag{2.3.23}$$

$$\sum_{n=1}^{\infty} a_n^{(1)}G_n^{(1)}(x) + \sum_{n=1}^{\infty} b_n^{(1)}H_n^{(1)}(x) = -p, \quad 0 < x < c\,. \tag{2.3.24}$$

Let $S_n(x)$ be an orthogonal set of functions satisfying the given conditions of orthogonality as

$$\int_0^c S_n(x)S_m(x)dx = N_n\delta_{nm}\,, \tag{2.3.25}$$

where $N_n = \int_0^c [S_n(x)]^2 dx$ and $S_n(x)$ can be constructed from an arbitrary set of functions say $G_n^{(1)}(x)$ such that

$$S_n(x) = \sum_{i=1}^{n} \frac{M_{in}}{M_{nn}} G_i^{(1)}(x), \tag{2.3.26}$$

where $S_1(x) = G_1^{(1)}(x)$ and $M'_{in}s$ are the cofactors of the elements m_{in} of M_n defined as

$$M_n = \begin{vmatrix} m_{11} & m_{12} & ... & m_{1n} \\ m_{21} & m_{22} & ... & m_{2n} \\ : & : & & : \\ m_{n1} & m_{n2} & ... & m_{nn} \end{vmatrix}, \qquad m_{in} = \int_0^c G_i^{(1)}(x)G_n^{(1)}(x)dx\,. \tag{2.3.27}$$

Let us rewrite the Eq.(2.3.24) in terms of the orthogonal series of $S_n(x)$ with coefficients c_n as

$$\sum_{n=1}^{\infty} a_n^{(1)} G_n^{(1)}(x) + p = \sum_{n=1}^{\infty} c_n S_n(x) = -\sum_{n=1}^{\infty} b_n^{(1)} H_n^{(1)}(x)\,. \tag{2.3.28}$$

Taking the second equality and using the condition for orthogonality of $S_n(x)$, we get

$$c_n = \sum_{n=1}^{\infty} \alpha_{ni} b_i^{(1)}, \tag{2.3.29}$$

where $\alpha_{ni} = -\frac{1}{N_n}\int_0^c S_n(x)H_i^{(1)}(x)dx$.

Taking the first equality, we get

$$a_n^{(1)} = \sum_{n=1}^{\infty} \gamma_{ni} b_i^{(1)}, \tag{2.3.30}$$

where $\gamma_{ni} = -\sum_{j=1}^{n} \frac{1}{N_j}\frac{M_{jn}}{M_{jj}}\int_0^c S_j(x)H_i^{(1)}(x)dx$.

Putting the value of $a_n^{(1)}$ in the Eq.(2.3.23), we get

$$\sum_{n=1}^{\infty}(\sum_{i=1}^{\infty}\gamma_{ni}b_i^{(1)})E_n^{(1)}(x)+\sum_{n=1}^{\infty}b_n^{(1)}F_n^{(1)}(x)=-\,p \tag{2.3.31}$$

$$or,\quad \sum_{n=1}^{\infty}b_n^{(1)}(\sum_{i=1}^{\infty}\gamma_{ni})E_n^{(1)}(x)+\sum_{n=1}^{\infty}b_n^{(1)}F_n^{(1)}(x)=-\,p \tag{2.3.32}$$

$$or,\quad \sum_{n=1}^{\infty}b_n^{(1)}Y_n^{(1)}(x)=-\,p, \tag{2.3.33}$$

where $Y_n^{(1)}(x)=\sum_{i=1}^{\infty}\gamma_{ni}E_n^{(1)}(x)+F_n^{(1)}(x)$.

Following the similar procedure towards the orthogonalization of the series given in Eq.(2.3.33) with the help of another orthogonal set of functions $T_n(x)$ given by

$$T_n(x)=\sum_{i=1}^{n}\frac{L_{in}}{L_{nn}}Y_i^{(1)}(x),$$

satisfying the orthogonality relation

$$\int_0^c T_n(x)T_m(x)dx=W_n\delta_{nm}\,,$$

with $W_n=\int_0^c[T_n(x)]^2dx$, we get

$$b_n^{(1)}=\sum_{j=n}^{\infty}\eta_j\frac{L_{jn}}{L_{jj}}, \tag{2.3.34}$$

where $\eta_j=-\frac{1}{W_j}\int_0^c pT_j(x)dx$ *and* $L'_{jn}s$ are the cofactors of the elements l_{in} of L_n , which is given by

$$L_n=\begin{vmatrix} l_{11} & l_{12} & \dots & l_{1n}\\ l_{21} & l_{22} & \dots & l_{2n}\\ \vdots & \vdots & & \vdots\\ l_{n1} & l_{n2} & \dots & l_{nn}\end{vmatrix},\qquad l_{in}=\int_0^c Y_i^{(1)}(x)Y_n^{(1)}(x)dx.$$

Now substituting $b_n^{(1)}$ in Eq.(2.3.30) , we will get $a_n^{(1)}$.These $a_n^{(1)}$ and $b_n^{(1)}$ are used in Eq.(32) to find the expression of $\sigma_{yy}^{(1)}(x,0)$.
For large value of ζ, the valueR^L can be evaluated by using the expression, $R(\zeta)/\zeta\rightarrow R^L$ i.e.,

$$R^L = R(\zeta_l)/\zeta_l, \tag{2.3.35}$$

where ζ_l is considered to be very large value of ζ.
Eq.(2.3.35) and the following relations:

$$\int_0^\infty J_n(xz)\{\cos(yz), \sin(yz)\}dz = [\cos\{n\sin^{-1}(y/x)\}, \sin\{n\sin^{-1}(y/x)\}] \\ /(x^2-y^2)^{1/2}, \qquad for\, x > y, \tag{2.3.36}$$

$$\int_0^\infty J_n(xz)\{\cos(yz), \sin(yz)\}dz = \{-x^n\,\sin(n\pi/2), x^n\,\cos(n\pi/2)\} \\ /[(y^2-x^2)^{1/2}\{y+(y^2-x^2)^{1/2}\}^n]\,, \; for\, y > x, \tag{2.3.37}$$

yield the expressions of $E_n^{(1)}(x), F_n^{(1)}(x), G_n^{(1)}(x)$ and $H_n^{(1)}(x)$ as

$$E_n^{(1)}(x) = \frac{(2n-1)}{\pi}[\int_0^\infty \left(R(\zeta)/\zeta - R^L\right) J_{2n-1}(a\zeta)\cos(\zeta x)d\zeta \\ + R^L\cos\{(2n-1)\sin^{-1}(x/a)\}/(a^2-x^2)^{1/2}], \tag{2.3.38}$$

$$F_n^{(1)}(x) = \frac{1}{2\pi}[\int_0^\infty \left(R(\zeta)/\zeta - R^L\right) J_n(\lambda_1\zeta)[\cos(n\pi/2)\{\sin(\lambda_2\zeta)+\sin(\lambda_3\zeta)\} \\ - \sin(n\pi/2)\{\cos(\lambda_2\zeta)+\sin(\lambda_3\zeta)\}]d\zeta + R^L\lambda_1^n[1/[(\lambda_2^2-\lambda_1^2)^{1/2}\{\lambda_2 \\ + (\lambda_2^2-\lambda_1^2)^{1/2}\}^n] + 1/[(\lambda_3^2-\lambda_1^2)^{1/2}\{\lambda_3+(\lambda_3^2-\lambda_1^2)^{1/2}\}^n]], \tag{2.3.39}$$

$$G_n^{(1)}(x) = \frac{(2n-1)}{\pi}[\int_0^\infty \left(R(\zeta)/\zeta - R^L\right) J_{2n-1}(a\zeta)\cos(\zeta x)d\zeta \\ + R^L(-1)^{(2n-1)}a^{2n-1}\sin\{(2n-1)\pi/2)\}/[(a^2-x^2)^{1/2}\{x \\ + (x^2-a^2)^{1/2}\}^{2n-1}]], \tag{2.3.40}$$

$$H_n^{(1)}(x) = \frac{1}{2\pi}[\int_0^\infty \left(R(\zeta)/\zeta - R^L\right) J_n(\lambda_1\zeta)[\cos(n\pi/2)\{\sin(\lambda_2\zeta)+\sin(\lambda_3\zeta)\} \\ - \sin(n\pi/2)\{\cos(\lambda_2\zeta)+\sin(\lambda_3\zeta)\}]d\zeta + R^L[\lambda_1^n/[(\lambda_2^2-\lambda_1^2)^{1/2}\{\lambda_2 \\ + (\lambda_2^2-\lambda_1^2)^{1/2}\}^n] + \sin\{n\sin^{-1}(\lambda_3/\lambda_1) - n\pi/2\}/[(\lambda_1^2-\lambda_3^2)^{1/2}]], \tag{2.3.41}$$

where $\lambda_1 = (c-b)/2$, $\lambda_2 = (c+b+2x)/2$, $\lambda_3 = (c+b-2x)/2$.

2.4 Stress intensity factor

The dynamic Mode I stress intensity factors at the tips of the cracks are obtained as

$$K_{Ia} = \lim_{x\to a^+} \sqrt{2\pi(x-a)}\sigma_{yy}^{(1)}(x,0) = \sum_{n=1}^{\infty} a_n^{(1)}(2n-1)(-1)^n R^L/2(\pi a)^{1/2}, \tag{2.4.1}$$

$$K_{Ib} = \lim_{x\to b^-} \sqrt{2\pi(b-x)}\sigma_{yy}^{(1)}(x,0) = \sum_{n=1}^{\infty} b_n^{(1)} R^L/(2\pi(c-b))^{1/2}, \tag{2.4.2}$$

$$K_{Ic} = \lim_{x\to c^+} \sqrt{2\pi(x-c)}\sigma_{yy}^{(1)}(x,0) = \sum_{n=1}^{\infty} b_n^{(1)}(-1)^{n-1} R^L/(2\pi(c-b))^{1/2}. \tag{2.4.3}$$

The stress magnification factor (SMF) at the crack tip $x = a$ can be determined by

$$M_{Ia} = \frac{K_{Ia}}{K_{Ia}^*}, \tag{2.4.4}$$

where K_{Ia}^* is stress intensity factor at $x = a$ due to presence of central crack only.

2.5 Numerical results and discussion

During numerical calculation, the composite materials Graphite epoxy and E-glass epoxy have been used as medium 1 and medium 2, whose material properties are given in Table 2.1.

Composite Materials	C_{11}	C_{22}	C_{12}	C_{66}	ρ
Graphite epoxy (Medium-I)	155.36	16.31	3.67	7.48	1.60
E-glass epoxy (Medium-II)	46.09	12.60	2.86	5.50	2.10

Table 2.1: Engineering material constants

The dimensionless SIFs have been calculated using the expression from Eqs (2.4.1)-(2.4.3) for different depths ($h = 2, 4$ and 6) of the orthotropic strip.The SIF at tip of the central crack is calculated keeping $a = 0.5, c = 1$ and $b = 0.6, 0.7, 0.8$. The SIFs at the outer crack tip are found keeping $b = 0.6$, $c = 1$ and $a = 0.2, 0.3, 0.4$. The variations of normalised SIFs $K_{Ia}/p\sqrt{\pi a}$, $K_{Ib}/p\sqrt{\pi(c-b)/2}$, $K_{Ic}/p\sqrt{\pi(c-b)/2}$ at $x = a, x = b, x = c$ against the wave numbers are shown through Figs. 2.2 - 2.4, Figs. 2.5 - 2.7 , Figs. 2.8 - 2.10, respectively for different crack lengths and depths of the medium 1.

It is seen from the figures that K_{Ia} decreases with the increase in the depth of

the orthotropic strip and also when the outer crack is moving away from the central crack. Again SIFs K_{Ib} and K_{Ic} both decrease with the increase in the depth of the strip and both increase when the distance between the central and outer cracks decrease.Here the values of K_{Ic} are less than the values of K_{Ib}.

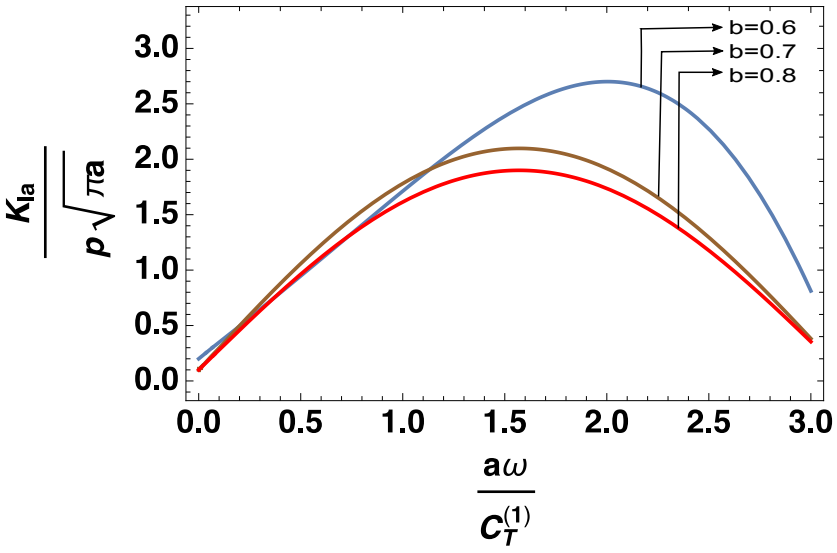

Figure 2.2: Variations of the normalised K_{Ia} vs. $a\omega/C_T^{(1)}$ for $a = 0.5, b = 0.6, 0.7, 0.8$ and $c = 1$ when $h = 2$.

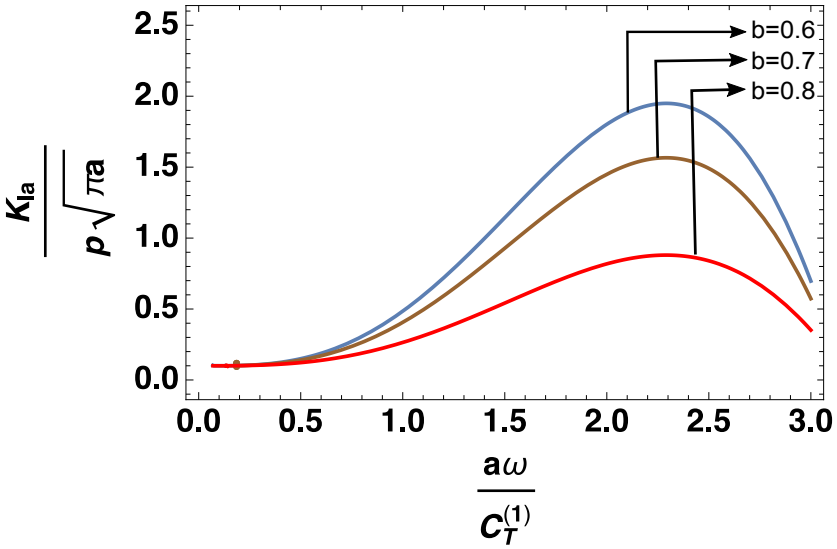

Figure 2.3: Variations of the normalised K_{Ia} vs. $a\omega/C_T^{(1)}$ for $a = 0.5, b = 0.6, 0.7, 0.8$ and $c = 1$ when $h = 4$.

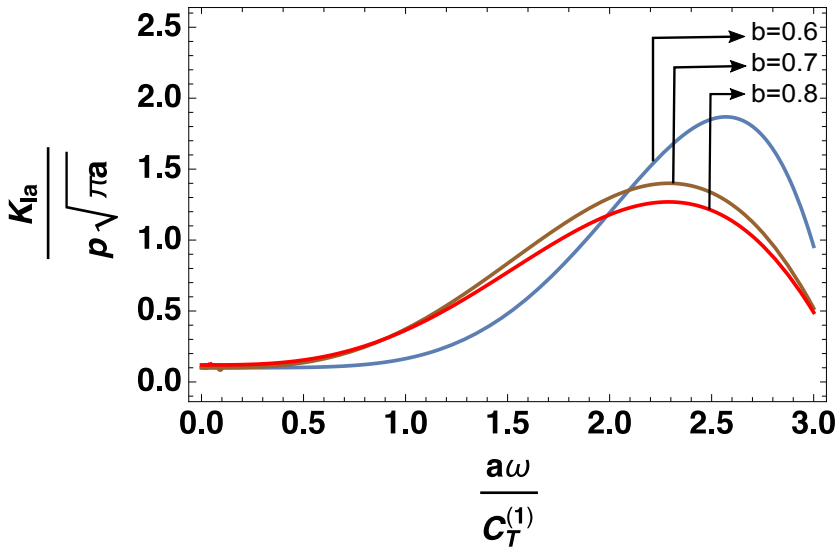

Figure 2.4: Variations of the normalised K_{Ia} vs. $a\omega/C_T^{(1)}$ for $a = 0.5, b = 0.6, 0.7, 0.8$ and $c = 1$ when $h = 6$.

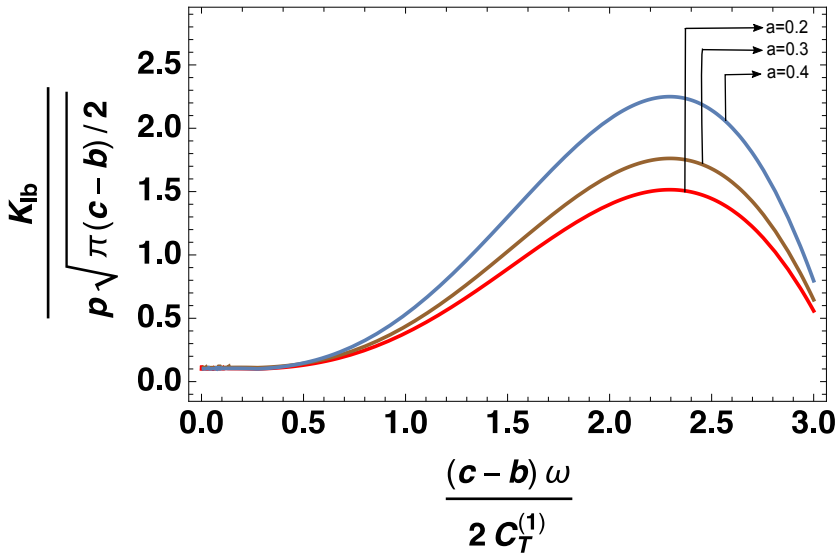

Figure 2.5: Variations of the normalised K_{Ib} vs. $(c - b)\omega/2C_T^{(1)}$ for $a = 0.2, 0.3, 0.4$, $b = 0.6$, $c = 1$ when $h = 2$.

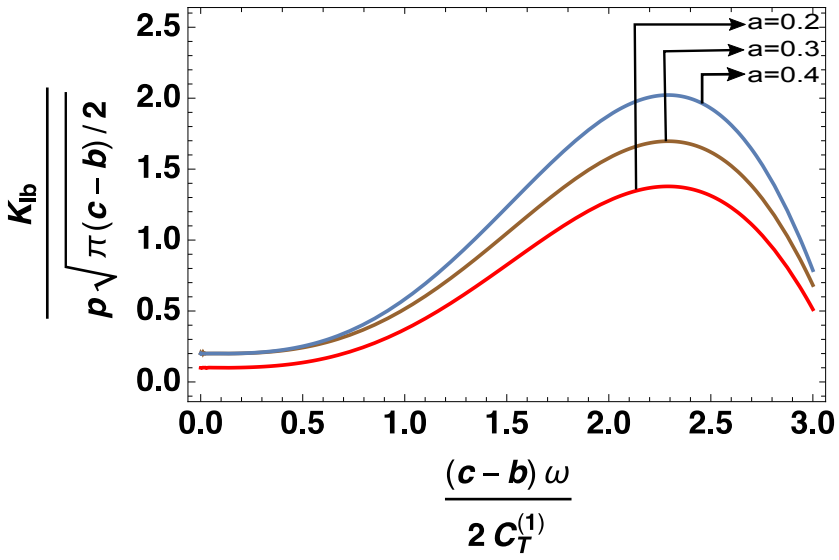

Figure 2.6: Variations of the normalised K_{Ib} vs. $(c-b)\omega/2C_T^{(1)}$ for $a = 0.2, 0.3, 0.4$, $b = 0.6$, $c = 1$ when $h = 4$.

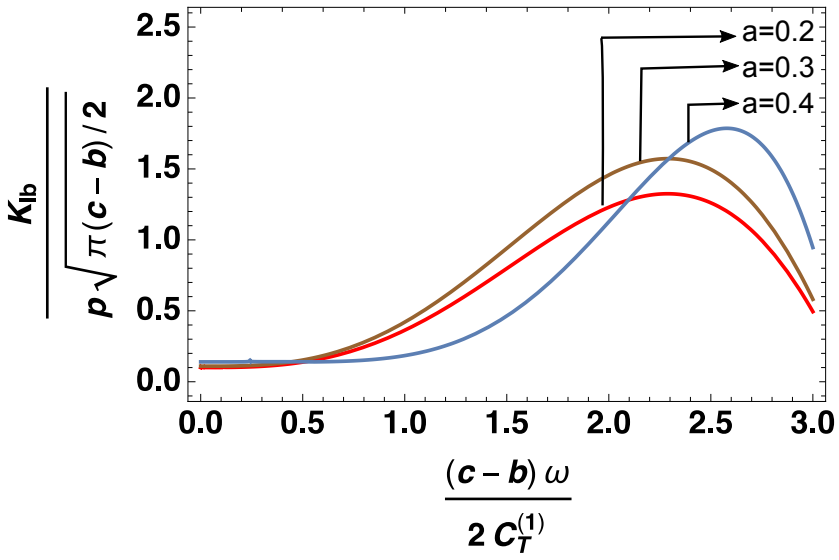

Figure 2.7: Variations of the normalised K_{Ib} vs. $(c-b)\omega/2C_T^{(1)}$ for $a = 0.2, 0.3, 0.4$, $b = 0.6$, $c = 1$ when $h = 6$.

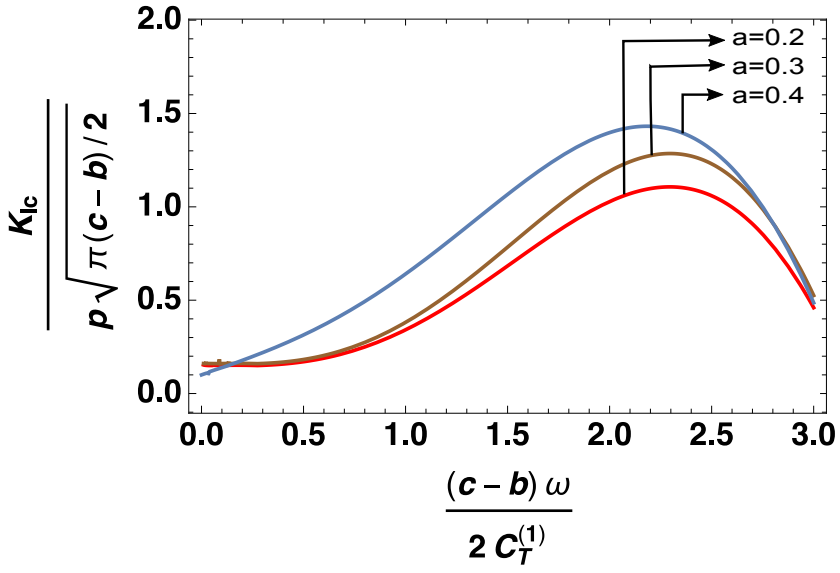

Figure 2.8: Variations of the normalised K_{Ic} vs. $(c-b)\omega/2C_T^{(1)}$ for $a = 0.2, 0.3, 0.4$, $b = 0.6$, $c = 1$ when $h = 2$.

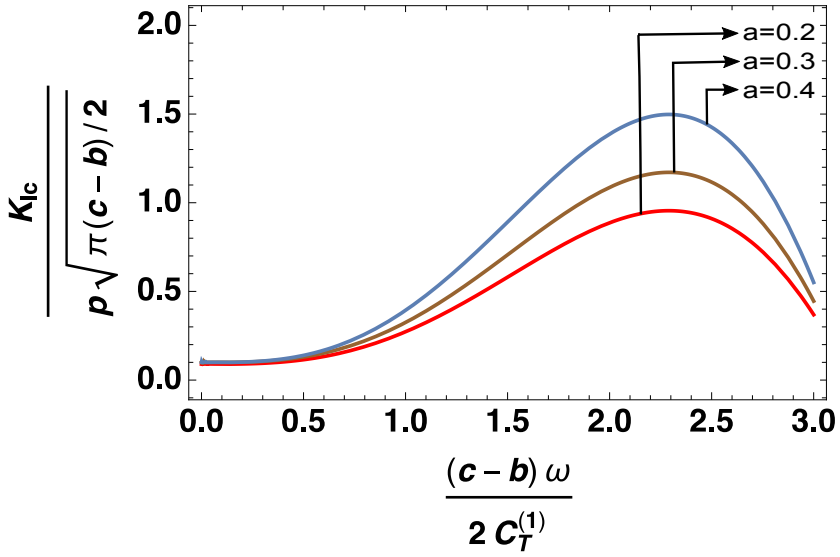

Figure 2.9: Variations of the normalised K_{Ic} vs. $(c-b)\omega/2C_T^{(1)}$ for $a = 0.2, 0.3, 0.4$, $b = 0.6$, $c = 1$ when $h = 4$.

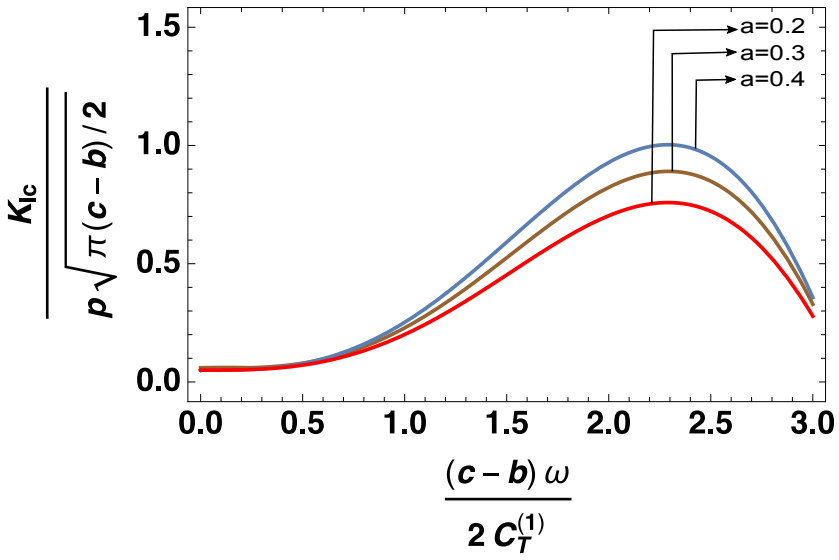

Figure 2.10: Variations of the normalised K_{Ic} vs. $(c-b)\omega/2C_T^{(1)}$ for $a = 0.2, 0.3, 0.4$, $b = 0.6$, $c = 1$ when $h = 6$.

Again it is seen that for each case the SIF increases with increase in wave number and then decreases.In each case overshoot is found.The peaks are higher for $h = 2$ while it decrease as the values of h increase.

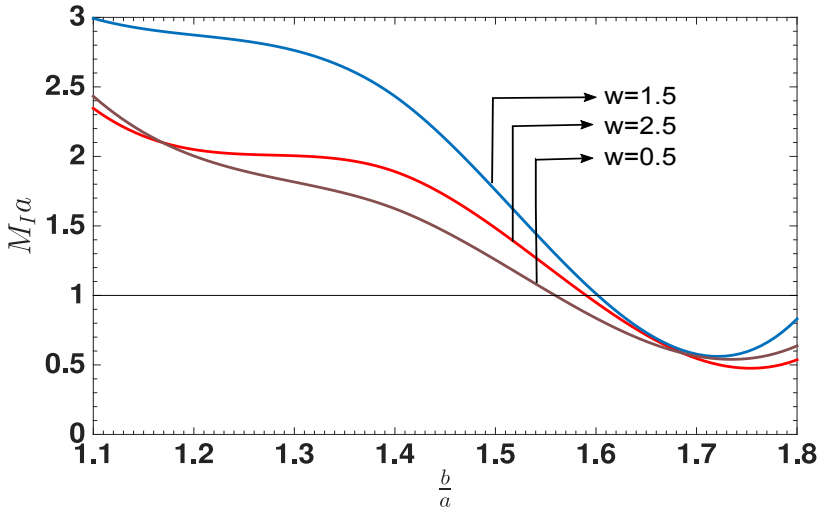

Figure 2.11: Variations of the M_{Ia} vs. b/a for different values of wave number (w) at $h = 2$.

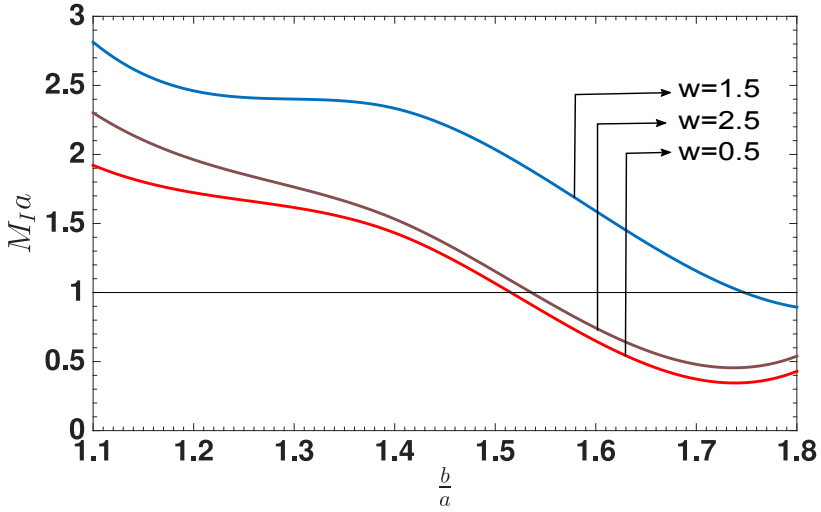

Figure 2.12: Variations of the M_{Ia} vs. b/a for different values of wave number (w) at $h = 4$.

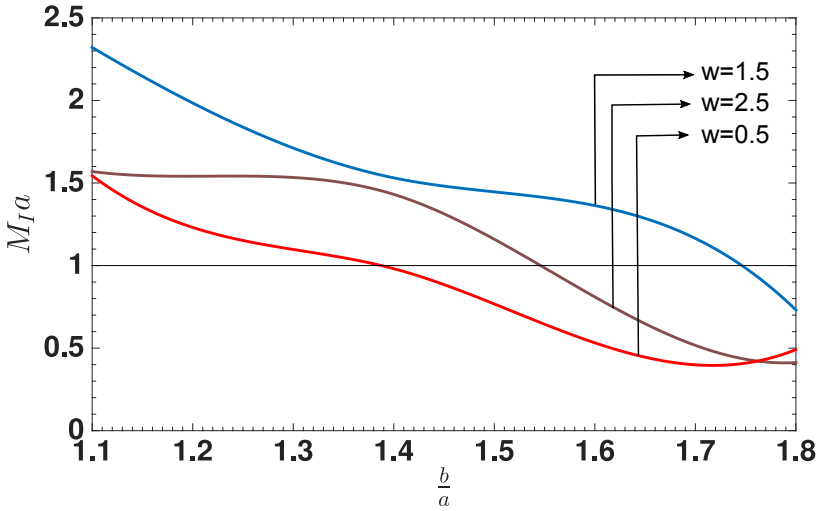

Figure 2.13: Variations of the M_{Ia} vs. b/a for different values of wave number (w) at $h = 6$.

The numerical values of the SMF given in the Eq. (2.4.4) are calculated for various wave numbers and different depths of the strip. The variations of the SMF against b/a keeping $c = 1$ are depicted through Fig. 2.11, Fig.2.12, Fig. 2.13 for $h = 2, h = 4$ and $h = 6$ respectively.The beauty of the physical quantity SMF (M_{Ia}) is that if $M_{Ia} < 1$, then shielding occurs i.e., there will be a possibility of crack arrest while $M_{Ia} > 1$ implies the occurrence of the amplification and as a result crack tip will propagate.

It is seen from the Figs.2.11-2.13 that if the central crack tip is fixed at $a = 0.5$

and the outer crack length is decreased i.e., the cracks' separation distance increases then there is a possibility of arrest of the central crack. If the depth of the strip (medium 1) increases, the possibility increases. It is also seen that the values of M_{Ia} will be higher for the wave number w= $a\omega/C_T^{(1)} = 1.5$. Thus for our considered model if the depth of the strip is small and cracks' separation distance is less then the tendency of propagating the tip of the central crack will be maximum for w=1.5.

2.6 Conclusion

This chapter succeeds in achieving three major goals:

- Initially, under time-harmonic waves impinging normal to the crack surfaces, determining the approximate analytical expressions of the SIFs at the tips of collinear cracks and stress magnification factor for central crack.
- The graphical depiction of the variations in normalized SIFs with respect to dimensionless wave numbers for various central and outer crack lengths as well as various depths of the strip.
- As the Stress magnification factor shows the shielding effect, which gives the possibilities for the central crack arrest because of the existence of the outer cracks.